

# Superscaling analyses, lepton scattering and nucleon momentum distributions in nuclei

A.N. Antonov<sup>1</sup>, M.V. Ivanov<sup>1</sup>, M.K. Gaidarov<sup>1</sup>, J.A. Caballero<sup>2</sup>, M.B. Barbaro<sup>3</sup>,  
and E. Moya de Guerra<sup>4</sup>

<sup>1</sup>Institute for Nuclear Research and Nuclear Energy, Bulgarian Academy of Sciences,  
Sofia 1784, Bulgaria

<sup>2</sup>Departamento de Física Atomica, Molecular y Nuclear, Universidad de Sevilla,  
Apdo. 1065, 41080 Sevilla, Spain

<sup>3</sup>Dipartimento di Fisica Teorica, Università di Torino and INFN, Sezione di Torino,  
Via P. Giuria 1, 10125 Torino, Italy

<sup>4</sup>Departamento de Física Atomica, Molecular y Nuclear, Facultad de Ciencias Físicas,  
Universidad Complutense de Madrid, Madrid E-28040, Spain

## Abstract

It is shown that superscaling is due to the high-momentum tail of the nucleon momentum distribution  $n(k)$  which is similar for all nuclei and is caused by the short-range and tensor nucleon-nucleon correlations. It is pointed out also that superscaling gives information about the general power-law asymptotics of  $n(k)$  and the nucleon-nucleon forces in the nuclear medium. The Coherent Density Fluctuation Model (CDFM) is used to calculate the total, longitudinal and transverse scaling functions on the basis of the hadronic tensor and the corresponding response functions in the RFG model. The results show a good agreement with the data and superscaling of the scaling function  $f(\psi')$  for negative  $\psi'$  including the region  $\psi' < -1$ , where the RFG model fails. The CDFM scaling functions are used to calculate the cross sections of the quasielastic (QE) electron scattering on nuclei in the mass region  $12 < A < 208$ , as well as charge-changing and neutral current neutrino (antineutrino) scattering on  $^{12}\text{C}$  in the QE and the  $\Delta$ -resonance regions at energies from 1 to 2 GeV.

## 1 Introduction

Over the past four decades electron scattering has provided important information on nuclear structure and dynamics. Form factors and charge distributions have been extracted from elastic scattering data, whereas inelastic measurements have been allowed for a systematic study of the dynamic response over a broad range of momentum ( $q$ ) and energy ( $\omega$ ) transfer. The scaling analyses of inclusive electron scattering from a large variety of nuclei (see e.g. [1, 2] for  $y$ -scaling and [3–8] for  $\psi'$ -scaling and superscaling) showed the evidence for the existence of high-momentum components of the nucleon momentum distribution  $n(k)$  at momenta  $k > 2 \text{ fm}^{-1}$ . It has been shown that it is due to the presence of nucleon-nucleon (NN) correlations in nuclei (for reviews, see e.g. [9]). It has been pointed out that this specific feature of  $n(k)/A$  is similar for all nuclei, and that it is a physical reason for the scaling and superscaling phenomena in nuclei. The latter is related to the independence of the reduced cross section on the momentum transfer  $q$  (scaling of first kind) and the mass number  $A$  (scaling of second kind). As known, the mean-field approximation (MFA) is unable to describe simultaneously the two important characteristics of the nuclear ground state, the density and momentum distribution. Therefore, a consistent and simultaneous analyses of the role of the NN correlations on both quantities is required using theoretical methods beyond the MFA in the description of relevant phenomena, e.g. those of the scaling ones. Such a possibility appears in the Coherent Density Fluctuation Model (CDFM) [9, 10] and this will be considered in the present work.

## 2 Superscaling and general properties of the nucleon momentum distribution and the NN forces in medium

The scaling variable  $\psi'$  has been introduced and superscaling considered in [3, 4] on the basis of the relativistic Fermi gas (RFG) model. However, the scaling function in this model is  $f(\psi') = 0$  for  $\psi' \leq -1$ , whereas the experimental scaling function extracted from  $(e, e')$  data extends up to  $\psi' \approx -2$ , where the effects beyond the MFA become important. Even more, it has been shown in [11] that the behavior of the scaling function  $f(\psi')$  for  $\psi' < -1$  depends on the particular form of the power-law asymptotic of  $n(k)$  at large  $k$  related to a corresponding behavior of the in-medium NN forces around the core [12]:

$$n(k) \xrightarrow{k \rightarrow \infty} \left[ \frac{\tilde{V}_{\text{NN}}(k)}{k^2} \right]^2, \quad (1)$$

where  $\tilde{V}_{\text{NN}}(k)$  is the Fourier transform of the NN interaction  $V_{\text{NN}}(r)$ . In principle, it is shown in the hard-sphere dilute Fermi gas [13, 14] that  $n(k)$  decrease like  $\sim 1/k^{4+m}$  [14], where  $m > 0$ . Using this, in [11] we obtained the following expression for the scaling function

$$f(\psi') = 0.12 \left( \frac{1+m}{2+m} \right) \frac{1}{|\psi'|^{2+m}} \quad (2)$$

that thus exhibits superscaling. Fitting the value of  $m$  from (2) to the experimental data for  $f(\psi')$  (see Fig. 1) one can see that the agreement with the scaling function is achieved when the value of  $m$  is in the interval  $4 \leq m \leq 5$ . The inverse Fourier transform of  $\tilde{V}_{\text{NN}}(k)$  gives  $V_{\text{NN}}(r) \sim \frac{1}{r}$  and  $V_{\text{NN}}(r) \sim \frac{1}{r^{1/2}}$  for  $m = 4$  and  $m = 5$ , respectively. Thus, the result obtained in [11] implies that inclusive quasielastic (QE) electron scattering from nuclei provides important information about the particular power-law form of the asymptotic of  $n(k)$  and on the NN forces in the nuclear medium.

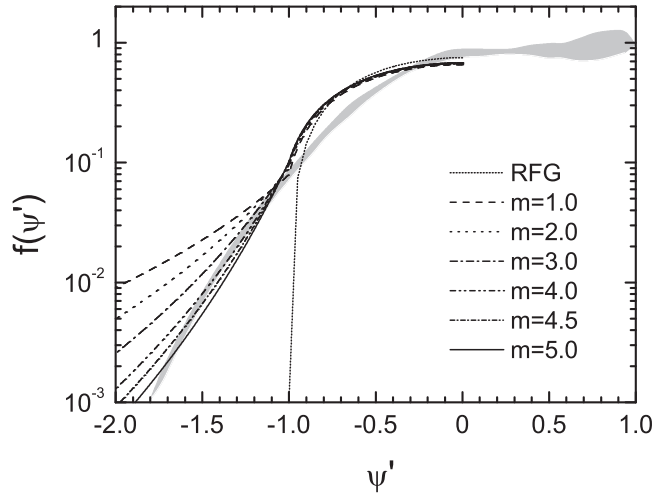


**Fig. 1:** The scaling function in a dilute Fermi gas calculated using Eq. (2) for different values of  $m$  in the asymptotics of the momentum distribution  $n(k) \sim 1/k^{4+m}$  given in comparison with the RFG result. The grey area shows experimental data taken from [6].

## 3 CDFM approach (I)

The drawback of the RFG model to describe the scaling function at  $\psi' < -1$  and the more general results from [11] have shown the necessity of considering the superscaling on the basis of a more complex dynamical picture of realistic finite nuclear systems beyond the RFG and MFA. So, as a particular example, in the first version of the CDFM approach (which is a natural extension of the Fermi gas model based on

the generator coordinate method [15] and includes long-range correlations (LRC) of collective type) the scaling function is obtained [7] on the basis of the RFG scaling function:

$$f_{\text{CDFM}_I}(\psi') = \int_0^{\alpha/(k_F|\psi'|)} |F(x)|^2 f_{\text{RFG}}(\psi', x) dx, \quad \text{where } f_{\text{RFG}}(\psi', x) \simeq \frac{3}{4} \left[ 1 - \left( \frac{k_F x |\psi'|}{\alpha} \right)^2 \right], \quad (3)$$

$$|F(x)|^2 = -\frac{1}{\rho_0(x)} \frac{d\rho(r)}{dr} \Big|_{r=x} \quad \text{at } \frac{d\rho(r)}{dr} \leq 0, \quad \text{or} \quad |F(x)|^2 = -\frac{3\pi^2}{2} \frac{\alpha}{x^5} \frac{dn(k)}{dk} \Big|_{k=\alpha/x} \quad \text{at } \frac{dn(k)}{dk} \leq 0 \quad (4)$$

with

$$\alpha = \left( \frac{9\pi A}{8} \right)^{1/3} \simeq 1.52A^{1/3}, \quad \rho_0(x) = \frac{3A}{4\pi x^3}, \quad k_F(x) = \frac{\alpha}{x}, \quad \text{and } k_F = \int_0^\infty k_F(x) |F(x)|^2 dx, \quad (5)$$

$\rho(\vec{r})$  and  $n(\vec{k})$  being normalized to  $A$ , and  $|F(x)|^2$  to unity.

#### 4 CDFM approach (II)

In contrast to the CDFM<sub>I</sub>, in this work and in [16] a more general CDFM approach (CDFM<sub>II</sub>) was developed starting not from the scaling function, but from the hadronic tensor, the response functions and related quantities in the RFG model with a density  $\rho_0(r)$  and a Fermi momentum  $k_F(x)$ , weighting the RFG model ones by the function  $|F(x)|^2$  (Eq. (4)) [16]:

$$W_{\text{CDFM}}^{\mu\nu} = \int_0^\infty |F(x)|^2 W_{\text{RFG}}^{\mu\nu}(x) dx, \quad (6)$$

$$R_L(\psi) = \int_0^\infty |F(x)|^2 R_L^{\text{(RFG)}}(x, \psi) dx, \quad R_T(\psi) = \int_0^\infty |F(x)|^2 R_T^{\text{(RFG)}}(x, \psi) dx, \quad (7)$$

where  $W_{\text{RFG}}^{\mu\nu}(x)$  and  $R_{L,T}^{\text{(RFG)}}(x, \psi)$  are those for the RFG [3] with a density  $\rho_0(x)$ ,  $\eta_F(x) = \frac{k_F(x)}{m_N}$ ,  $\varepsilon_F(x) = \sqrt{1 + \eta_F^2(x)}$  and the scaling variable  $\psi$  is:  $\psi \equiv \frac{1}{\sqrt{\xi_F}} \frac{\lambda - \tau}{\sqrt{(1 + \lambda)\tau + \kappa\sqrt{\tau(1 + \tau)}}$ , where

$\xi_F = \sqrt{1 + \eta_F^2} - 1$ ,  $\lambda = \frac{\omega}{2m_N}$ ,  $\kappa \equiv \frac{q}{2m_N}$ ,  $\tau = \kappa^2 - \lambda^2$ . Then the total, longitudinal  $L$ , and transverse  $T$  scaling functions are obtained by:

$$f^{\text{CDFM}_{II}}(\psi) = k_F \times \frac{C^{\text{CDFM}}(\psi)}{S}, \quad f_L(\psi) = k_F \times \frac{R_L(\psi)}{G_L}, \quad f_T(\psi) = k_F \times \frac{R_T(\psi)}{G_T}, \quad (8)$$

where

$$C^{\text{CDFM}}(\psi) \equiv \frac{d^2\sigma}{d\Omega d\varepsilon'} = \sigma_M \left\{ \left( \frac{Q^2}{q^2} \right)^2 R_L(\psi) + \left[ \frac{1}{2} \left| \frac{Q^2}{q^2} \right| + \tan^2 \frac{\theta}{2} \right] R_T(\psi) \right\}, \quad (9)$$

$$S = \sigma_M \left\{ \left( \frac{Q^2}{q^2} \right)^2 G_L(\tau) + \left[ \frac{1}{2} \left| \frac{Q^2}{q^2} \right| + \tan^2 \frac{\theta}{2} \right] G_T(\tau) \right\} \quad (10)$$

is the single-nucleon  $eN$  elastic cross section [17] with the single-nucleon functions  $G_L$  and  $G_T$  being expressed by the proton and neutron electric and magnetic Sachs form factors [3, 16] and  $k_F$  is calculated using Eq. (5).

## 5 Results of calculations on scaling functions and electron- and neutrino-nuclei scattering cross sections

We present firstly our results of longitudinal [Fig. 2(a)] and transverse [Fig. 2(b)] scaling functions at fixed values of momentum transfer  $q = 0.3, 0.5, 0.8$  and  $1.0$  GeV/c calculated within the CDFM<sub>II</sub> approach compared with results of the relativistic plane-wave impulse approximation (RPWIA) with Lorentz gauge [18]. In contrast with our previous results, where the CDFM<sub>I</sub> scaling functions are equal,  $f_L^{\text{CDFM}_I}(\psi) = f_T^{\text{CDFM}_I}(\psi) = f^{\text{CDFM}_I}(\psi)$ , and do not depend on the momentum transfer  $q$ , in the CDFM<sub>II</sub> the scaling functions depend on the momentum transfer  $q$  till a sufficiently high  $q$ . As can be seen from Fig. 2, scaling of first kind is clearly violated for low  $q$  values ( $q < 0.5$  GeV/c) in the negative  $\psi$  region, whereas for  $q$  of the order of  $0.5$  GeV/c, scaling violation slowly disappears as  $q$  increases and the CDFM<sub>II</sub> and RPWIA scaling functions reach their asymptotic values. The result for the total quasielastic scaling function can be seen in the next Fig. 3, where we present our results of calculations of  $f^{\text{QE}}(\psi)$  [Eq. (8)] for  $^{12}\text{C}$  within the CDFM<sub>II</sub> model for  $q = 0.3 - 1.0$  GeV/c with a step of  $0.1$  GeV/c. Note that the asymmetry in the scaling function, clearly observed for low  $q$  values, tends to disappear as  $q$  goes up.

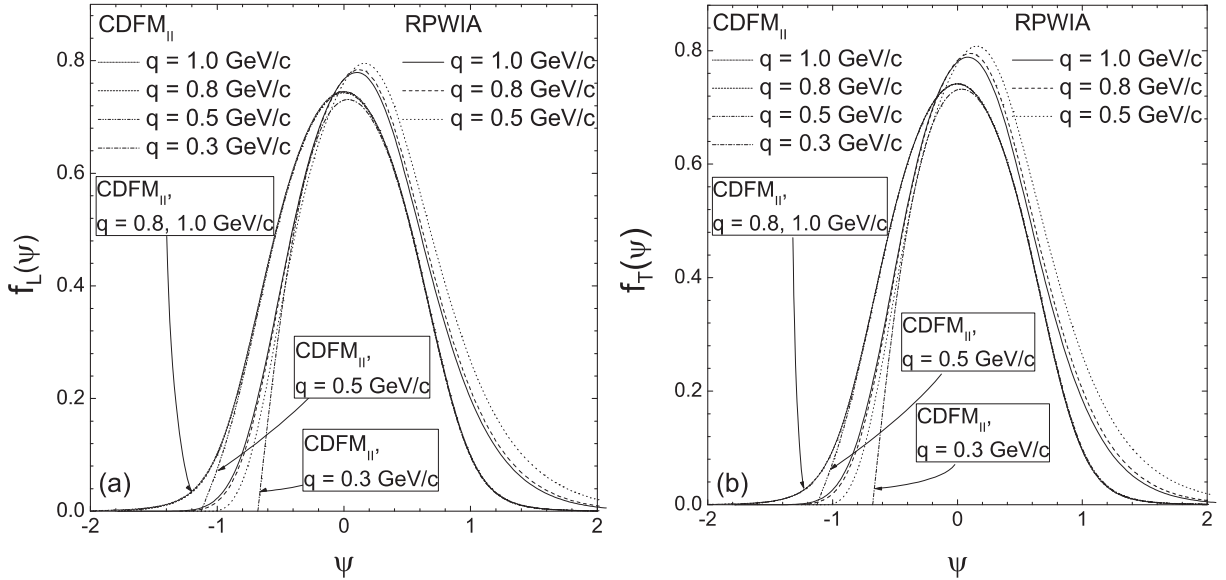


**Fig. 2:** The longitudinal scaling functions  $f_L(\psi)$  (a) and the transverse scaling functions  $f_T(\psi)$  (b) for  $^{12}\text{C}$  calculated in the CDFM<sub>II</sub> for  $q = 0.3, 0.5, 0.8,$  and  $1.0$  GeV/c and RPWIA (Lorentz gauge) for  $q = 0.5, 0.8,$  and  $1.0$  GeV/c.

In Fig. 4 we present results for the ratio  $f_L(\psi)/f_T(\psi)$  for  $^{12}\text{C}$  calculated in the CDFM<sub>II</sub> and RPWIA (Lorentz gauge) at fixed values of momentum transfer  $q = 0.3, 0.5, 0.8,$  and  $1.0$  GeV/c. In the CDFM<sub>II</sub> calculations we observe violation of the scaling of the zeroth kind [ $f_L(\psi) \neq f_T(\psi)$ ], at variance with the CDFM<sub>I</sub> one. The behavior of the ratio  $f_L(\psi)/f_T(\psi)$  in our model is similar to that in the RPWIA for positive  $\psi$  values where the response is positive except for very low  $q$  ( $q = 0.3$  GeV/c), while in the negative  $\psi$  region, the ratio  $f_L(\psi)/f_T(\psi)$  becomes negative for RPWIA and positive for CDFM<sub>II</sub>.

The next step in our studies is to examine the scaling of the second kind in the CDFM<sub>II</sub>. This requires calculations of the scaling functions for different nuclei. In Fig. 5 we give the results for the quasielastic scaling functions for  $^{12}\text{C}$ ,  $^{27}\text{Al}$ ,  $^{56}\text{Fe}$ , and  $^{197}\text{Au}$  calculated in the CDFM<sub>I</sub> and CDFM<sub>II</sub>, respectively. The result of the RFG model is also presented. One can see the essential difference between the results of the RFG model and those of the CDFM<sub>I</sub> and CDFM<sub>II</sub> in the region  $\psi' < -1$ . It can be seen also from our results that the scaling of the second kind is good in the CDFM. The behavior of the CDFM<sub>I</sub> and CDFM<sub>II</sub> scaling functions can be explained by the long-range collective correlations included in the

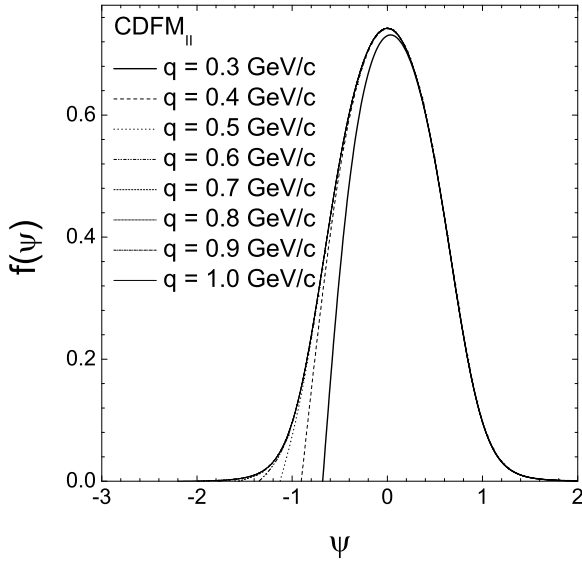


**Fig. 3:** The quasielastic scaling function  $f^{\text{QE}}(\psi)$  for  $^{12}\text{C}$  calculated in the CDFM<sub>II</sub> for  $q = 0.3 - 1.0$  GeV/c with step 0.1 GeV/c.

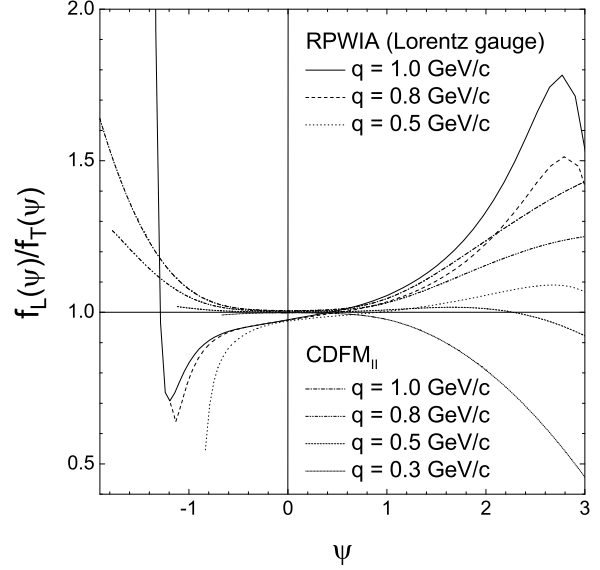


**Fig. 4:** The ratio  $f_L(\psi)/f_T(\psi)$  for  $^{12}\text{C}$  calculated in the CDFM<sub>II</sub> for  $q = 0.3, 0.5, 0.8,$  and  $1.0$  GeV/c and RPWIA (Lorentz gauge) for  $q = 0.5, 0.8,$  and  $1.0$  GeV/c.

CDFM. These correlations are important and they are reflected in the tail of the CDFM scaling functions at negative  $\psi'$ . In contrast, the results of mean-field approaches (relativistic or not) are generally closer to those of the RFG model. We note that the difference between the CDFM scaling function and that from the RFG model for  $|\psi'| > 1$  which can be seen in Fig. 5 is due to the large difference between  $n(k)$  in CDFM and that in the RFG model, where the (dimensionless) momentum distribution is a step function.

A test of the CDFM superscaling functions is performed (Fig. 6) by calculations of the cross sections of electron scattering in quasielastic and  $\Delta$ -region for nuclei with  $12 \leq A \leq 208$  at different energies and angles using the CDFM<sub>I</sub> and CDFM<sub>II</sub> scaling functions. For the scaling function in the  $\Delta$ -region we use our approach from Ref. [7]. As can be seen from Fig. 6 the results calculated with both CDFM<sub>I</sub> and CDFM<sub>II</sub> scaling functions do not differ too much, agreeing well with experimental data in the QE region. Away from the QE and  $\Delta$ -peaks the behavior of the cross sections is due to higher resonances. We also display the separate longitudinal and transverse contributions to the QE peak.

The features of superscaling in inclusive electron-nucleus scattering have made it possible to initiate analyses of neutrino and antineutrino scattering off nuclei on the same basis (e.g. [17,20]). Neutrino-(antineutrino-) nucleus charge-changing (CC) [20] or neutral-current (NC) [21] scattering cross sections for intermediate to high energies can be calculated by multiplying the elementary single-nucleon CC or NC neutrino (antineutrino) cross sections by the corresponding scaling functions. These assumptions have been tested within the relativistic mean-field (RMF) plus final-state interaction (FSI) model [22]. A number of other theoretical studies of CC and NC neutrino (antineutrino)-nucleus scattering has been performed in recent years (for references see, e.g. [16,20–26]). In the present work (see also [27] and [16]) we applied the CDFM QE- and  $\Delta$ -scaling functions to the calculations of charge-changing neutrino-nucleus scattering following the formalism given in [17]. In Fig. 7 we present the CDFM results for the cross section of the charge-changing neutrino ( $\nu_\mu, \mu^-$ ) reaction on  $^{12}\text{C}$  at  $\theta_\mu = 45^\circ$  and  $\varepsilon_\nu = 1$  GeV. The calculations are performed using not only the CDFM<sub>I</sub> but also the CDFM<sub>II</sub> quasielastic scaling function. In the figure we present also the result (labeled “CDFM<sub>II</sub> (asymmetric)”) achieved by introducing, as done in our previous work [8], a phenomenological asymmetric tail of the superscaling function at  $\psi > 0$ . Our results are compared with those from RFG model, SuSA and RPWIA approaches. We note that the result for the CDFM<sub>II</sub> with asymmetry is closer to that calculated using the phenomenological

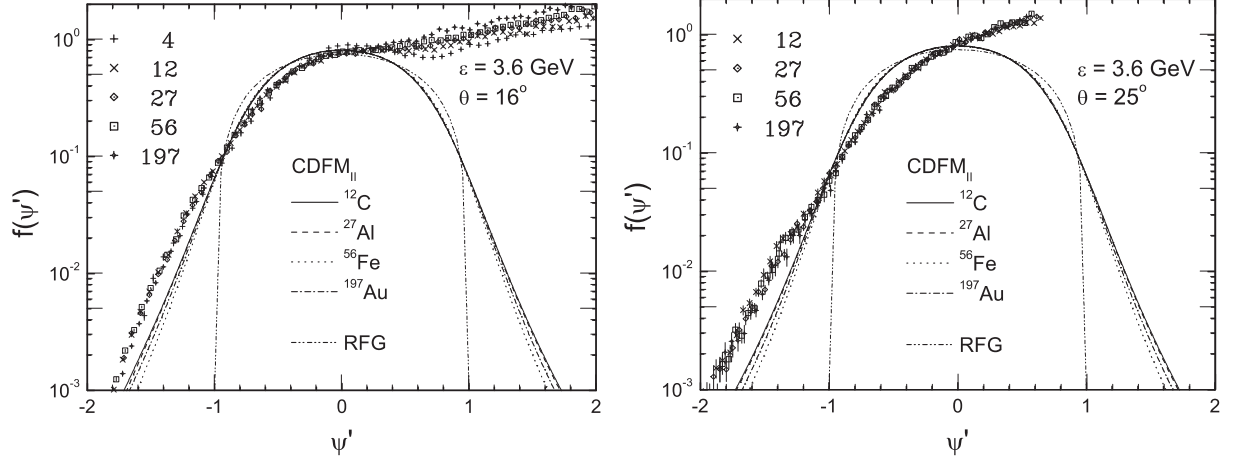


**Fig. 5:** The quasielastic scaling function  $f^{QE}(\psi')$  for  $^{12}\text{C}$ ,  $^{27}\text{Al}$ ,  $^{56}\text{Fe}$ , and  $^{197}\text{Au}$  calculated in the CDFM<sub>I</sub> and RFG. The experimental data are taken from [5, 6] and the labels indicate the mass number for each set of data.

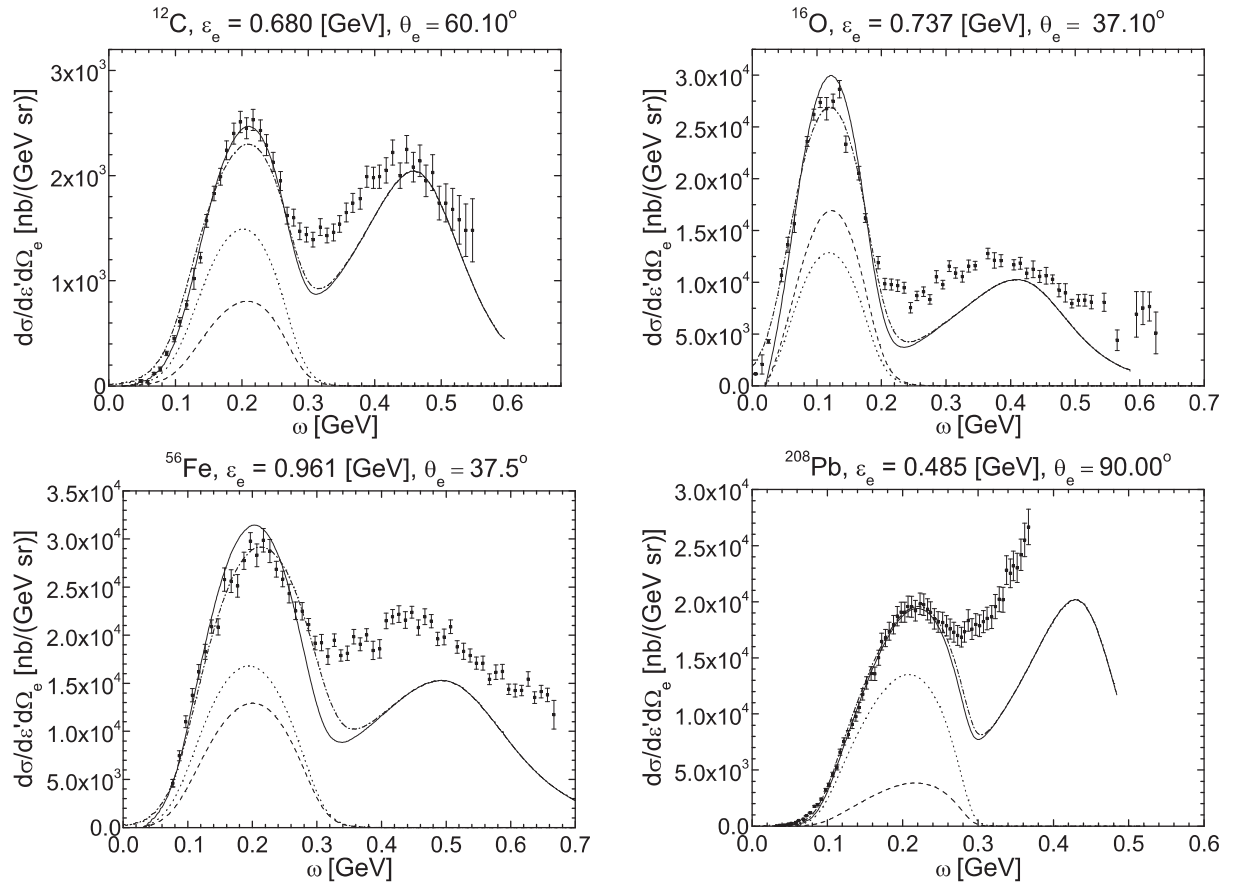


**Fig. 6:** Inclusive electron cross sections as function of energy loss. The results are given: the CDFM<sub>I</sub> dash-dotted line, the CDFM<sub>II</sub> solid line, the  $L$ -contribution in CDFM<sub>II</sub> dashed line, the  $T$ -contribution in CDFM<sub>II</sub> dotted line. The experimental data are taken from [19].

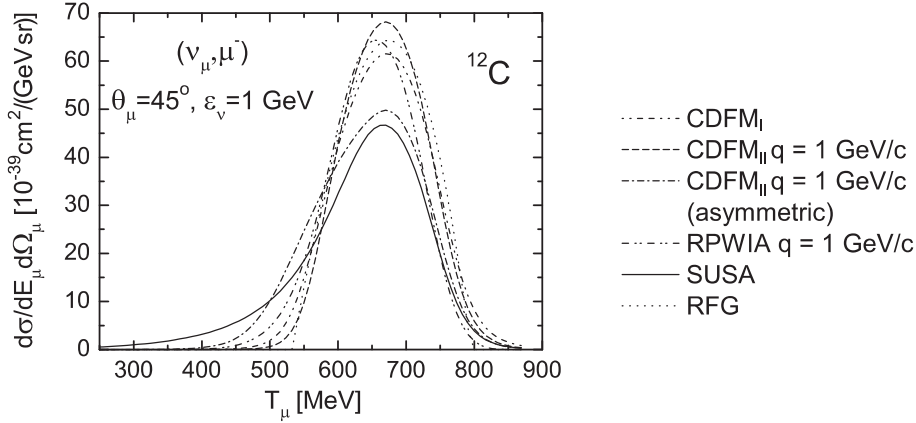


**Fig. 7:** The cross section of charge-changing neutrino ( $\nu_\mu, \mu^-$ ) reaction on  $^{12}\text{C}$  at  $\theta_\mu = 45^\circ$  and  $\varepsilon_\nu = 1$  GeV.

(SuSA) scaling function that is extracted from the experimental data on inclusive electron scattering. However, CDFM<sub>I</sub> and CDFM<sub>II</sub> models lead to very close results, with the maximum of the scaling function being slightly higher in the latter. The scaling functions for both approaches follow closely the behavior exhibited by the RPWIA one.

The CDFM approach was also applied in this work (see also [23]) to calculate QE scattering via the weak neutral current of neutrinos and antineutrinos from nuclei, using the basic formalism from [21].

## 6 Conclusions

The results of the present work can be summarized as follows:

- A new, more general, approach within the Coherent Density Fluctuation Model is proposed (CDFM<sub>II</sub>). We apply it to calculate the total  $f(\psi)$ , the longitudinal  $f_L(\psi)$  and the transverse  $f_T(\psi)$  scaling functions by taking as starting point the hadronic tensor and the longitudinal and transverse response functions in the RFG model. The approach leads to a slight violation of the zero-kind scaling [ $f_L(\psi) \neq f_T(\psi)$ ] in contrast with the situation in the RFG and CDFM<sub>I</sub> models. It is found that the ratio  $f_L(\psi)/f_T(\psi)$  in the CDFM<sub>II</sub> has similarities with that from the RPWIA approach (with Lorentz gauge) for positive  $\psi$ . It is shown that the CDFM<sub>II</sub> scaling functions calculated for different values of the transferred momentum  $q$  show a saturation of its asymptotic behavior. Scaling of first kind appears at  $q$  larger than  $\approx 0.5$  GeV/c.
- The CDFM scaling functions are applied to calculate cross sections of inclusive electron scattering (and their longitudinal and transverse components) in the quasielastic and  $\Delta$ -regions for nuclei with  $12 \leq A \leq 208$  at different energies and angles. The results are in good agreement with available experimental data, especially in the QE region.
- The CDFM<sub>II</sub> approach is applied to calculate charge-changing neutrino (antineutrino) scattering on  $^{12}\text{C}$  at 1 GeV incident energy. The results are compared with those from the RFG model, as well as from the SuSA and RPWIA approaches. The CDFM scaling function is also applied to calculate QE scattering via the weak neutral current of neutrinos (antineutrinos) from nuclei.

## Acknowledgements

This work was partly supported by the Bulgarian National Science Fund under contracts nos DO 02–285 and  $\Phi$ –1501 and by Ministerio de Educación y Ciencia (Spain) under contract nos. FPA2006–13807–C02–01, FIS2005–01105, FIS2005–00640, FIS2008–04189, and PCI2006–A7–0548, and the Spanish Consolider-Ingenio 2010 programme CPAN (CSD2007–00042). This work is also partially supported by the EU program ILIAS N6 ENTApP WP1. M.V.I. acknowledges support from the European Operational programm HRD through contract BGO051PO001/07/3.3–02/53 with the Bulgarian Ministry of

Education. M.B.B. and J.A.C. acknowledge support from the INFN-MEC agreement, project “Study of relativistic dynamics in neutrino and electron scattering”.

## References

- [1] G. B. West, *Phys. Rep.* **18** (1975) 263; I. Sick, D. B. Day, and J. S. McCarthy, *Phys. Rev. Lett.* **45** (1980) 871.
- [2] C. Ciofi degli Atti and G. B. West, *Phys. Lett. B* **458** (1999) 447 (and references therein).
- [3] W. M. Alberico, A. Molinari, T. W. Donnelly, E. L. Kronenberg, and J. W. Van Orden, *Phys. Rev. C* **38** (1988) 1801.
- [4] M. B. Barbaro, R. Cenni, A. De Pace, T. W. Donnelly, and A. Molinari, *Nucl. Phys.* **A643** (1998) 137.
- [5] T. W. Donnelly and I. Sick, *Phys. Rev. Lett.* **82** (1999) 3212.
- [6] T. W. Donnelly and I. Sick, *Phys. Rev. C* **60** (1999) 065502.
- [7] A. N. Antonov, M. K. Gaidarov *et al.*, *Phys. Rev. C* **69** (2004) 044321; *Phys. Rev. C* **71** (2005) 014317.
- [8] A. N. Antonov, M. V. Ivanov *et al.*, *Phys. Rev. C* **73** (2006) 047302; *Phys. Rev. C* **74** (2006) 054603.
- [9] A. N. Antonov, P. E. Hodgson, and I. Zh. Petkov, *Nucleon Momentum and Density Distributions in Nuclei* (Clarendon Press, Oxford, 1988); *Nucleon Correlations in Nuclei* (Springer-Verlag, Berlin-Heidelberg-New York, 1993).
- [10] A. N. Antonov, V. A. Nikolaev, and I. Zh. Petkov, *Bulg. J. Phys.* **6** (1979) 151; *Z. Phys. A* **297** (1980) 257; *ibid.* **304** (1982) 239; A. N. Antonov, D. N. Kadrev, and P. E. Hodgson, *Phys. Rev. C* **50** (1994) 164.
- [11] A. N. Antonov, M. V. Ivanov, M. K. Gaidarov, and E. Moya de Guerra, *Phys. Rev. C* **75** (2007) 034319.
- [12] R. D. Amado and R. M. Woloshyn, *Phys. Lett. B* **62** (1976) 253; *Phys. Rev. C* **15** (1977) 2200; R. D. Amado, *Phys. Rev. C* **14** (1976) 1264.
- [13] A. B. Migdal, *Sov. Phys. JETP* **5** (1957) 333; V. M. Galitskii, *Sov. Phys. JETP* **7** (1958) 104; V. A. Belyakov, *Sov. Phys. JETP* **13** (1961) 850; W. Czyż and K. Gottfried, *Nucl. Phys.* **21** (1961) 676.
- [14] R. Sartor and C. Mahaux, *Phys. Rev. C* **21** (1980) 1546; *Phys. Rev. C* **25** (1982) 677.
- [15] J. J. Griffin and J. A. Wheeler, *Phys. Rev.* **108** (1957) 311.
- [16] A. N. Antonov, M. V. Ivanov, M. B. Barbaro, J. A. Caballero, E. Moya de Guerra, *Phys. Rev. C* **79** (2009) 044602.
- [17] J. E. Amaro, M. B. Barbaro, J. A. Caballero, T. W. Donnelly, A. Molinari, and I. Sick, *Phys. Rev. C* **71** (2005) 015501.
- [18] J. A. Caballero, *Phys. Rev. C* **74** (2006) 015502.
- [19] O. Benhar, D. Day, and I. Sick, *Rev. Mod. Phys.* **80** (2008) 189.
- [20] J. A. Caballero, J. E. Amaro *et al.*, *Phys. Rev. Lett.* **95** (2005) 252502; J. E. Amaro, M. B. Barbaro *et al.*, *Phys. Rev. C* **71** (2005) 065501.
- [21] J. E. Amaro, M. B. Barbaro, J. A. Caballero, and T. W. Donnelly, *Phys. Rev. C* **73** (2006) 035503.
- [22] J. A. Caballero, J. E. Amaro, M. B. Barbaro, T. W. Donnelly, and J. M. Udias, *Phys. Lett. B* **653** (2007) 366.
- [23] A. N. Antonov, M. V. Ivanov, M. B. Barbaro, J. A. Caballero, E. Moya de Guerra, and M. K. Gaidarov, *Phys. Rev. C* **75** (2007) 064617.
- [24] A. Meucci, C. Giusti, and F. D. Pacati, *Nucl. Phys.* **A739** (2004) 277; *Nucl. Phys.* **A773** (2006) 250.
- [25] M. Martini, G. Co’, M. Anguiano, and A. M. Lallena, *Phys. Rev. C* **75** (2007) 034604.
- [26] T. Leitner, L. Alvarez-Ruso, and U. Mosel, *Phys. Rev. C* **74** (2006) 065502; K. S. Kim *et al.*, *J. Phys. G: Nucl. Part. Phys.* **34** (2007) 2643.
- [27] M. V. Ivanov, M. B. Barbaro, J. A. Caballero, A. N. Antonov, E. Moya de Guerra, and M. K. Gaidarov, *Phys. Rev. C* **77** (2008) 034612.